Clays and Clay Minerals, Vol. 44, No. 6, 801–810, 1996.

SUBMICROSCOPIC STRUCTURE OF Fe-COATINGS ON QUARTZ GRAINS IN TROPICAL ENVIRONMENTS

E. PADMANABHAN AND A. R. MERMUT

Department of Soil Science, University of Saskatchewan, Saskatoon, Saskatchewan, S7N 5A8, Canada

Abstract—Formation of Fe-coatings or segregation at the expense of quartz grains is a common process in the tropical environment. Limited information is available about their internal structure at the submicroscopic level. The transmission electron microscope (TEM) and energy dispersive X-ray microprobe analyses (EDXRMA) techniques were used to identify the nature and arrangement of fundamental mineral particles within the Fe-coatings. Chemical and mineralogical studies showed that the coatings were composed of well-crystallized Fe-oxides, quartz and kaolinite. The EDXRMA analyses revealed the presence of linear concentrations (laminae) of nearly pure Fe oxide along the edges and the contact zone with quartz and within the coatings. Similar atomic proportions of Al and Si in several areas within the interior regions of coatings and the XRD pattern of the crushed coatings are supportive evidence for the presence of kaolinite. Under the TEM, the dense laminae (<10 μm thick) consisted of elongated Fe-oxide particles (<1.5 μm long and 0.2 μm thick) accommodated in subparallel arrangement. The interior areas had very high porosity and, in addition to Fe-oxides, contained other minerals: mainly kaolinite, quartz and isolated areas of Al-oxides. High amounts of ultramicroscopic pores (<0.5 μm) in the interior region suggested that dissolution of Fe-oxides occurred under reduced conditions, with subsequent reprecipitation of pure Fe-oxides in the laminae. Very low porosity and parallel arrangement of Fe-oxide particles (laminae) provided new surfaces (barrier) for Fe-accumulation when soil solutions provided new influxes of iron, thereby creating a thicker Fe-coating. The size and geometry of the ultramicroporosity were shown to play a significant role in the dissolution and precipitation of soil minerals, especially those involved in redox reactions.

Key Words—Electron Microscopy, Fe-coating, Fe-nodules, Fe-oxide Forms, Submicroscopic Structure, Ultrathin Sections, X-ray Microprobe Analysis.

INTRODUCTION

Iron can accumulate in various forms in soils and sediments that experience alternating wet and dry periods, which not only favor redox processes, but also hydration and dehydration processes (Sherman and Kanehiro 1954; Brewer 1976; Arshad and St. Arnaud 1980). In many Oxisols, sand-size quartz grains are corroded and coated with Fe-oxides. In extreme cases, the entire quartz grain is replaced by Fe-oxides. Eswaran and Stoops (1979) pointed out that the corrosion of quartz, despite the fact that it is a slow reaction, could result in a steady supply of silica to the soil system.

It is known that the particle size and morphology of Fe-oxides are dependent on the precursor and conditions of transformation (Schwertmann et al. 1977; Lewis and Schwertmann 1979). Schwertmann and Taylor (1989) discuss the environments favoring the formation of various Fe-oxides. For example, silicate anions usually coexist with Fe-oxides and retard or inhibit the transformation of these minerals to more crystalline products (Herbillon and Tran 1969; Schwertmann 1985). Vempati et al. (1990) showed that the morphology of hematite synthesized from ferrihydrite is influenced by the presence of SiO_3^{2-}. Mobilization of Fe usually takes place through the reductive reactions. As the condition changes from that of reduction to oxidation, Fe may become immobilized (Krauskopf 1967).

Sposito and Reginato (1992) pointed out the importance of electron microscopic techniques, used in conjunction with the quantitative energy-dispersive X-ray spectral analysis, in evaluating the nature and behavior of soil minerals. They suggested that there is a major gap in understanding the composition of mixed solid-phase minerals, their size, morphology and arrangement in the soil matrix and the possible interactions with the soil solutions and biosphere. Research on the role of Fe-concentrations in adsorption of phosphorus (Taylor and Schwertmann 1974; Tiessen et al. 1991) and in the acceleration of iron pan formation by continuous rice paddy cultivation (Mohr et al. 1972) have shown the need for the expansion of knowledge on the fabric and mineralogical characteristics of these constituents.

Bruemmer et al. (1988) indicated that knowledge of porosity provided a better understanding of the problem of irreversibility of metal desorption hysteresis during adsorption-desorption reactions. Studies on the nature and arrangements of Fe-oxide accumulations have been performed using the scanning electron microscope (Cescas et al. 1970; Gallaher, Perkins and Radcliffe 1973; Gallaher, Perkins, Tan and Radcliffe 1973; Pawluk and Dumanski 1973; Eswaran et al. 1978), at relatively low magnifications. These workers

Table 1. Selected characteristics of the soil used in this study.

Depth (cm)	Horizon	pH (1:1) (soil : water)	CEC $cmol_c\ kg^{-1}$	Texture	OC	Fe_d†	Fe_t	Ti_t	Fe_o/Fe_t
		Soil 1				%			
0–12	A	4.1	8.3	scl‡	1.05	1.67	3.12	0.55	0.54
27–60	BA	5.0	5.4	scl‡	0.56	1.75	3.33	0.73	0.53
98–150	Bo2	5.4	3.2	scl‡	0.34	1.73	3.51	0.74	0.49

† DCB-extractable Fe, Fe_t and Ti_t = Total Fe and Ti in the untreated soil samples.
‡ Sandy clay loam. pH, CEC, texture and organic carbon from Santos et al. (1989).

observed definite zoning patterns for Fe, infilling of voids by Fe-oxides and the compact nature of the general matrix. Amouric et al. (1986) characterized Fe-oxyhydroxides and the accompanying phases in undisturbed samples of lateritic iron-crust pisolites, using the ion-milling technique and TEM to determine the internal structure and the processes that led to their formation. Detailed analyses of the internal structure of Fe-oxide concentrations, including coatings, at submicroscopic levels appear to be rare.

The objective of this study was to evaluate the submicroscopic structure within the Fe-coatings on quartz grains occurring in an Oxisol.

MATERIALS AND METHODS

A Haplustox from the Pernambuco state in Brazil was used for this study. The soil is developed on a Cretaceous sandstone and located on a gently sloping to nearly level plateau, at an elevation of about 900 m MSL. The area has a semi-arid climate with mean annual precipitation of 750 mm and mean annual temperature of 24 °C. The fractured, pitted (and, apparently, etched) sand-size quartz grains in the soil are generally coated and their cracks infilled, to various degrees, by Fe-oxides.

Quartz grains coated with Fe-oxides were hand-picked. The coatings were separated from the grains under a dissecting microscope and crushed to pass a 50-μm sieve. The organically complexed Fe (Fe_p) was determined using sodium pyrophosphate (Bascomb 1968), poorly crystalline Fe-oxides (Fe_o) (McKeague and Day 1966) and the well-crystalline Fe-oxides (Fe_d) (Mehra and Jackson 1960). Total elemental analyses were carried out using the HF digestion method (Jackson 1973). In the soil samples, the total Fe (Fe_t), total Ti (Ti_t) and dithionite-citrate bicarbonate (DCB) extractable Fe (Fe_d) were also determined by the same procedures. Mineralogical composition was determined by X-ray diffraction (XRD) techniques using a Philips diffractometer with an Fe tube. Liquid magnetic separation of the clay fractions was performed according to Ghabru et al. (1987). The Hinckley Index for kaolinite was determined according to Plançon et al. (1988). Organic carbon (OC) was analyzed using a Leco CR-12 Carbon System (Leco Corporation, Michigan) operated at 840 °C.

The coated grains used for this study were selected from the BA horizon (27–60 cm depth) of the soil, embedded in epoxy resin. They were cut and polished with diamond paste to avoid any contamination. Elemental mapping and line scans were carried out using EDXRMA attached to a JEOL JXA-8600 Superprobe (operated at 15 kV and 10 nA) with scanning electron microscope (SEM) ability. Oriented fragments of the Fe-coatings were selected using a binocular microscope and embedded in Spurr's resin (Spurr 1969; J.B.E.M. Services, Inc., Dorval, Quebec). Fe-coatings ≤2 mm thick were selected to obtain an intact ultracut approximately 150 μm thick with a diamond knife, using a microtome (Smart and Tovey 1982). TEM studies of the ultrathin sections were carried out using a Zeiss CM 10 TEM (Oberkochen, West Germany) operated at 120 kV.

RESULTS AND DISCUSSION

General Characteristics of the Soil

The soil has low pH, OC contents, cation exchange capacity (CEC) and total Fe and Ti, but has a uniform texture throughout the profile (Table 1). Iron and Ti increase slightly with depth. The DCB extracts (Fe_d) contained 49 to 54% of the total Fe. The soil is well-drained due to the presence of stable soil-microaggregates and large interaggregate pore spaces.

Chemical and Mineralogical Characteristics

The ground Fe-oxides coating has very low amounts of pyrophosphate (Fe_p) and oxalate (Fe_o) extractable Fe. The insignificant amounts of Fe_p are likely due to very low OC contents (Table 2) that favor the precipitation of hematite, as suggested by Schwertmann (1985). The DCB-extractable Fe (Fe_d) is about 41% of the total Fe content (Fe_t). Low Fe_o/Fe_d and Fe_d/Fe_t values show that the material is essentially composed of well-crystallized Fe-oxides. Lower solubility is also attributed to larger size of the ground materials. The DCB-extractable Ti (Ti_d) is very low, which suggests that Ti exists as discrete minerals. Total analyses of the coatings confirmed that, in addition to very high contents of Fe, Al and Si are also present (Table 2), implying the existence of phyllosilicates. The Si that is in excess of Al is probably due to the presence of quartz in the coatings.

Table 2. Chemical properties of the coating (average collected from a large number of grains).

Sample	%										
	OC	Fe_p	Fe_o	Fe_d	Ti_d	Fe_t	Al	Ti_t	Si	Fe_o/Fe_d	Fe_d/Fe_t
Coating	0.08	0.03	0.30	17.50	0.54	42.34	8.73	2.80	11.42	0.02	0.41

XRD (Figure 1) confirms that the ground materials comprise hematite (0.260 nm), kaolinite (0.72 nm) and quartz (0.428 and 0.336 nm). There appear to be no peaks for geothite. This is to be expected, since the Fe-coatings have formed over a long period of time under the dry soil moisture regime, which would encourage the transformation of geothite to hematite, as suggested by Schwertmann and Taylor (1989). The peaks for kaolinite are sharp and narrow in the XRD pattern of the crushed coatings.

Light Microscopy

Iron-oxide concentrations occur concentrically around grains of quartz (Bullock et al. 1985). The fractured quartz grains with Fe infillings are termed "runiquartz" (Eswaran et al. 1975). Under polarized light, the coatings are dark with distinct external boundaries. The enclosing soil microaggregates (Santos et al. 1989) have a similar color. Under plane-polarized light, the coatings appear to be somewhat darker than soil aggregates.

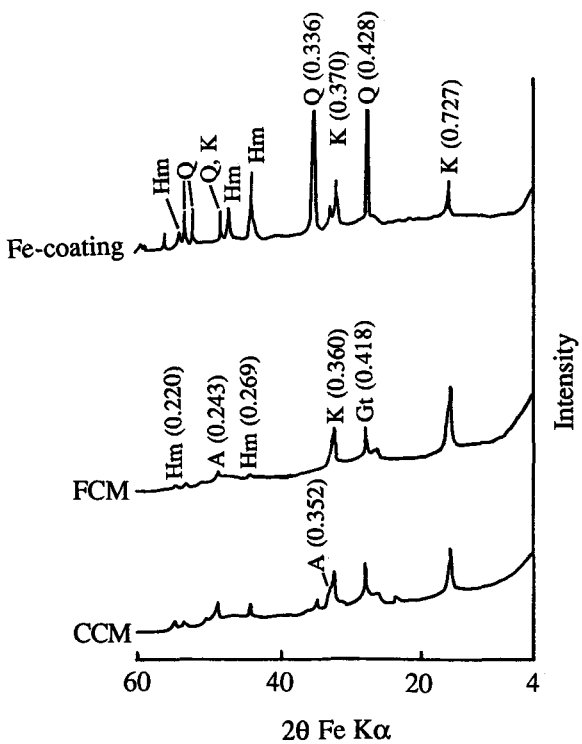

Figure 1. X-ray diffractograms of the powdered coatings in comparison with the fine-clay magnetic (FCM) and coarse-clay magnetic (CCM) fractions of the BA horizon in the soil used for this study (400 cps). Hm = hematite, Q = quartz, K = kaolinite, Gt = goethite, A = anatase.

SEM Observations

At low magnifications, the external surfaces of the coatings are smooth (Figure 2a), but, with higher magnifications, they appear to be pitted and exhibit some degree of porosity (Figures 2a and 2b). Back-scattered electron images of polished sections show that the thin accretionary layers (laminae) exhibit a concentric (Figure 3a) and cross-concentric internal morphology (Figures 3a and 3b), probably indicating interruptions in the development stages. The Fe-coatings are not in direct contact with the quartz grain, and there is a space between the 2 constituents. The quartz grain has numerous dissolution pits infilled to varying extents by clay-size particles, mostly of Fe-oxides, with somewhat accommodating arrangement.

The EDXRMA analyses revealed distinct laminae of Fe precipitates at the edges, within the coating and at the surfaces close to the quartz grain (Figures 4a and 4b). Small (< 2–3 μm) aggregates of Fe-oxides can also be observed within the coatings (Figures 4a through 4d). There is less Fe-oxide accumulation in the interlaminae regions. Several lines of evidence show that the Fe-coatings on the mineral surfaces are formed by diffusion of Fe to particle surfaces, following the weathering of Fe-bearing minerals (Cho and Mermut 1992).

Each lamina most likely represents a phase in the development of accretionary material. The soil is the origin of the basic supply of Fe. Quartz dissolution may take place in the soil in a slow but steady fashion (Eswaran et al. 1975). Quartz grains are likely to serve as nuclei for the concentration of Fe-oxides when there is enough Fe. The general grainy appearance of the interior part of the Fe-coating supports the view that this region has porosity and/or consists of minerals which are made up of light elements. Aluminum and Si distributions examined by EDXRMA show that, indeed, these elements are present within the coatings (Figures 4c and 4d) and do not occur in the laminae. The similarity in the distributions of Al and Si supports the XRD results and confirms that kaolinite is present in the interlaminae regions. As can be seen in Figures 4a, 4c and 4d, there are pockets that appear to be rich in kaolinite (indicated as "k" in Figures 4c and 4d). Such areas are less dense and probably represent trapped soil microaggegates. Silicon and Al distributions show that there are areas (thick and diffuse

https://doi.org/10.1346/CCMN.1996.0440611 Published online by Cambridge University Press

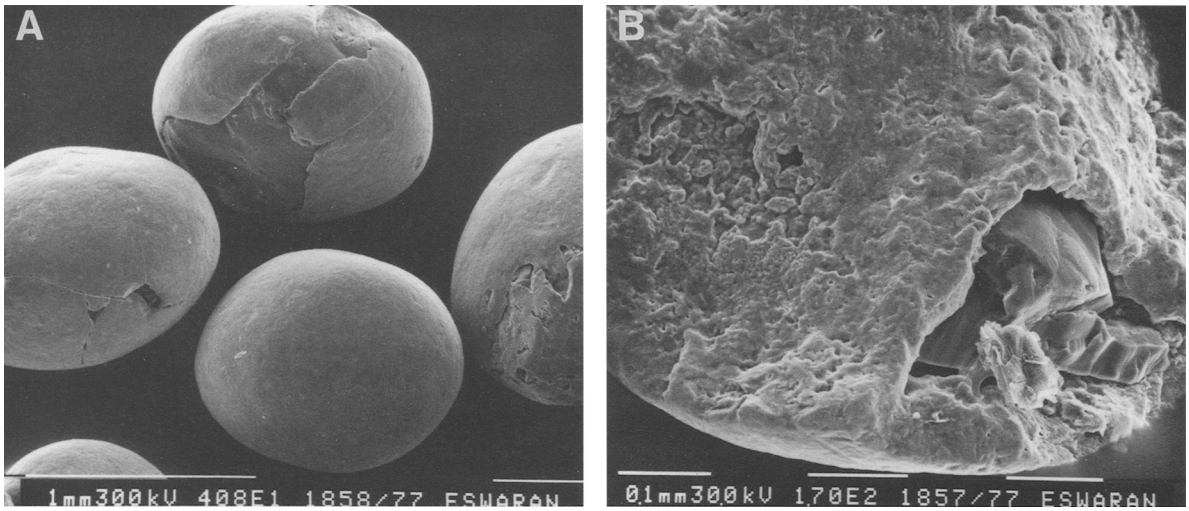

Figure 2. Scanning electron microscope micrographs of the coated quartz grains, showing: a) cracks and incomplete coatings; and b) pitted surface at higher magnifications and quartz grain with linear grooves and etch marks. Note the void between the quartz and the surrounding coating.

laminae) indicating a layer of probable kaolinitic clay coatings (Figures 4a, 4c and 4d).

The interior areas of the infillings within the quartz grain (corroded areas) also contain high concentrations of Al and Si. Locally, small pockets containing Al as a predominant element can also be found (Figure 4c), suggesting the presence of gibbsite. Titanium is found in discrete particles (Ti-bearing minerals) in the interlaminae regions (Figure 4e), implying that these particles were probably trapped with the clay particles during the accretionary process. Milnes and Fitzpatrick (1989) describe a variety of conditions under which Ti can be accumulated.

The similarity in the distributions of Al and Si in the EDXRMA line scans confirmed the presence of kaolinite (Figures 5a and 5b). Results of elemental analysis across the coating also indicate that the distribution patterns for Fe and Ti are different, supporting the previously mentioned view that Ti exists mostly as discrete mineral particles.

Ultrathin Sections

Under the TEM, 2 zones within the Fe-coatings, the dense laminae and interior regions, can easily be identified.

DENSE LAMINAE. This region (Figures 6a through 6c) comprises electron-dense, elongated hematite crystals. Some particles are kinked, despite the fact that they are in subparallel arrangement. The fundamental particles of this region are large (up to 1.5 μm in length) and exhibit face-to-face associations. The

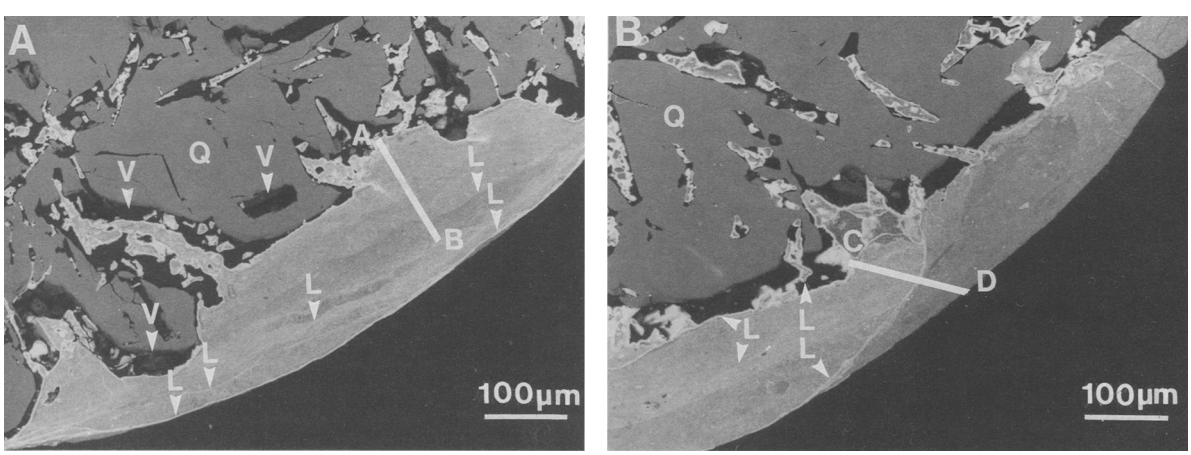

Figure 3. Back-scattered electron images of polished specimens: a) concentric laminae (L); and b) cross-concentric laminae. Note the dissolution pits (V) in quartz (Q) with infillings, and concentration of electron dense particles in the coatings (white spots). Note that A-B and C-D refer to line scans shown in Figure 5.

https://doi.org/10.1346/CCMN.1996.0440611 Published online by Cambridge University Press

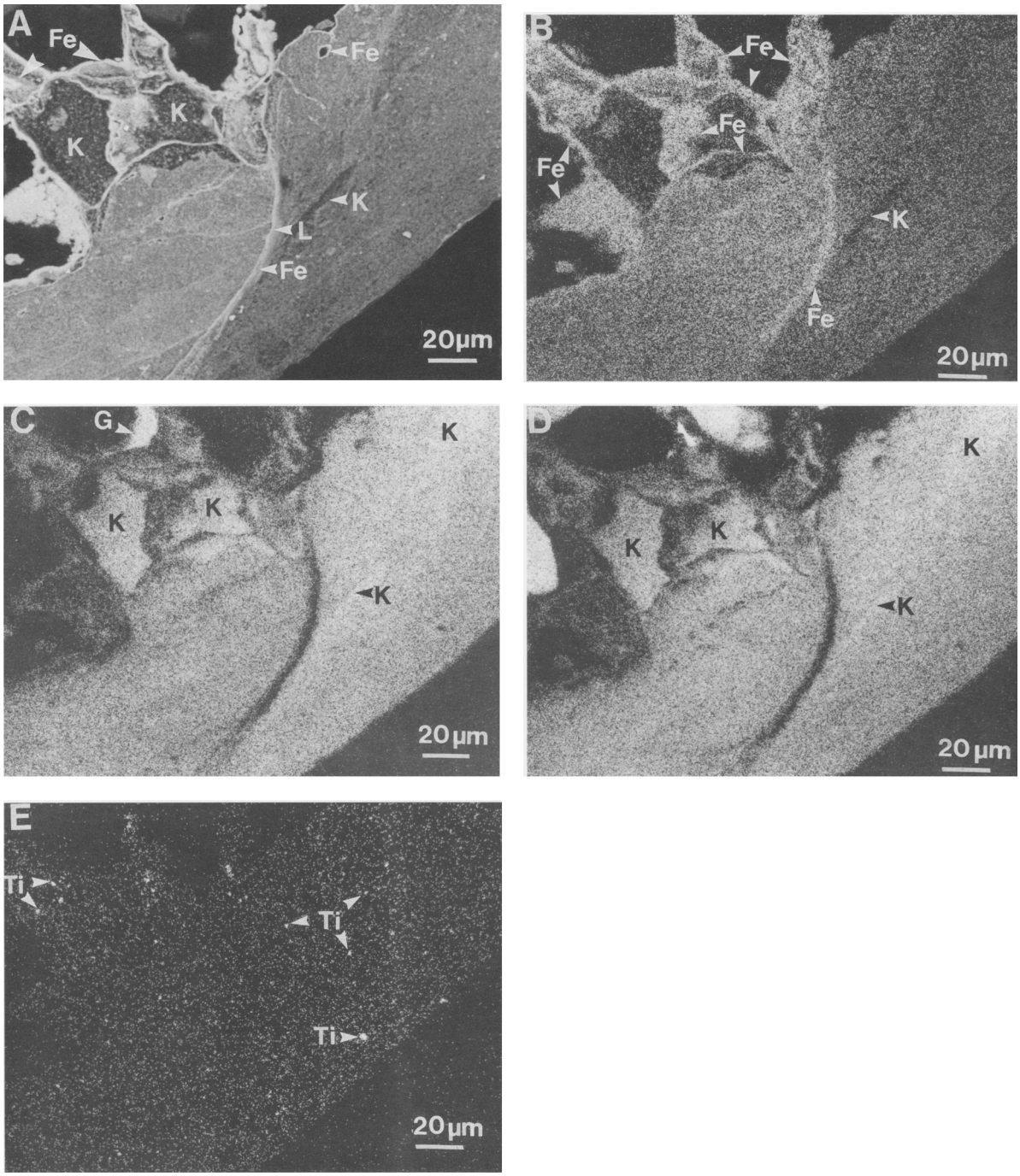

Figure 4. Selected X-ray microprobe micrographs of a coated quartz grain: a) back-scattered electron image of the Fe-coating; b) elemental distributions of Fe; c) Al; d) Si and e) Ti in that region. Fe = iron oxide, G = gibbsite, K = kaolinite, Ti = titanium.

particles are <200 nm thick and the entire thickness of the laminae is <10 µm. As mentioned previously, this zone consists of Fe-oxides with little or no Al (Figures 4 and 5). The large particle size supports the suggestion (Schwertmann et al. 1977) that Fe-oxides increase in particle size and have better crystallinity with decreasing amounts of Al substitution; this also favors hematite formation (Lewis and Schwertmann 1979; Schwertmann et al. 1979). In places, the sizes of the Fe-oxide particles are smaller than the rest of the laminae, suggesting continuous dissolution and precipitation with a possible

https://doi.org/10.1346/CCMN.1996.0440611 Published online by Cambridge University Press

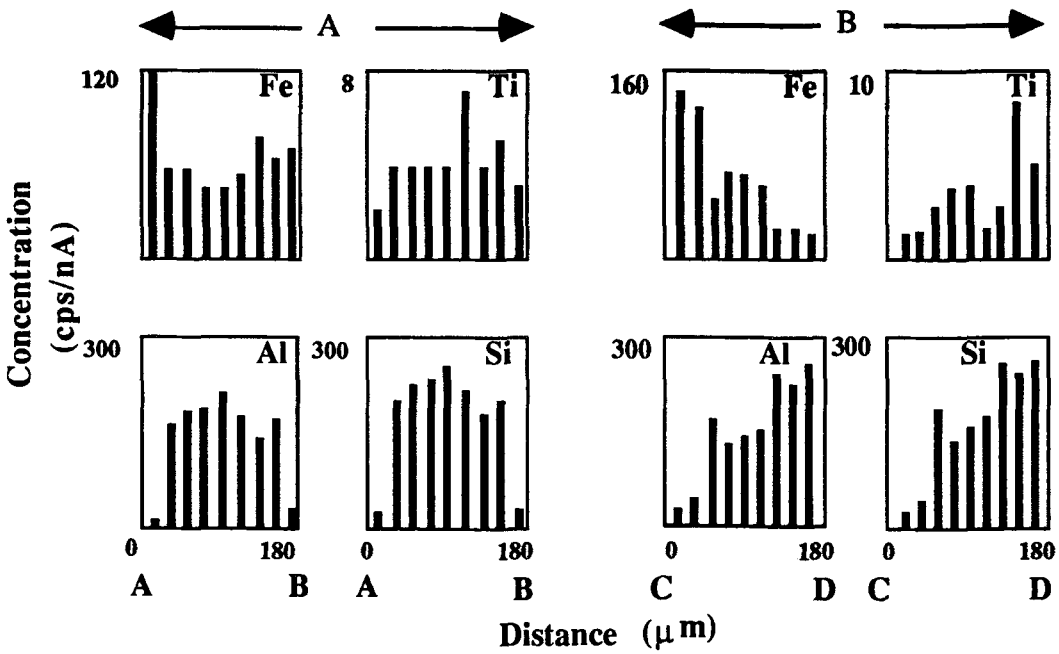

Figure 5. Energy dispersive X-ray line scans of the coatings in 2 regions: a) transect A-B (See Figure 3a); and b) transect C-D (see Figure 3b). Notice the dissimilarities in distributions of Fe and Ti. The elements Al and Si have a similar distribution and are concentrated between the laminae.

supply of Fe from the interior parts of the coating (Figures 6b through 6d).

The characteristic feature of this region is the dense packing arrangement of the fundamental particles. The very low porosity would reduce the infiltration of soil solutions into and from the nodules. Shadfan et al. (1985) stated that the hardness of Fe accretions depended on the mineralogy, content, crystallinity and mean crystallite dimension of the Fe-oxides. However, the arrangement of the fundamental particles is also an important factor determining the hardness.

Moving from the edge toward the interior, there are a few randomly distributed domains consisting of shorter Fe-oxide particles (hematite) and lighter particles (kaolinite and quartz), which are still arranged in a densely packed mode (Figure 6d). Several silicate minerals, such as kaolinite and quartz, coexist with hematite, suggesting that these particles are either trapped or neoformed in this environment. Well-crystallized kaolinite may have developed from the poorly crystallized precursor kaolinite. Tardy and Nahon (1985), Trolard and Tardy (1989) and Nahon (1991) have suggested that formation of kaolinite is possible within the Fe accretionary formations.

Other types of electron-dense particles were also detected, but these have different morphology and are not kinked like those in the laminae (Figure 7a). The particles are generally <0.5 μm in dimensions. Porosity increases with increasing distance from the laminae. The coexistence of kaolinite and hematite in the transition zones could be attributed to the increase in H_2O activity, which increases the stability of kaolinite and favors the precipitation of hematite (Tardy and Nahon 1985).

Another feature of the transition zones is the occurrence of domains within which particles are connected by a gel-like material (Figure 7b). This material has previously been interpreted as coatings of short-range-order oxides or oxyhydroxides of Fe, Al or Si (Jones and Uehara 1973), indicating hydrolysis processes that could have occurred with decreased H_2O activity (Tardy and Nahon 1985). The presence of such intermediate dissolution or precipitation products indicates a supply of Fe originating from the interior regions that appears to precipitate in the laminae.

THE INTERIOR REGION. This region consists predominantly of light minerals (kaolinite, quartz and Al-oxides) (Figures 7c and 7d). The Hinckley Index for the crushed coatings suggests that the kaolinite particles are well-crystallized. The principal difference in mineralogy between this region and those discussed earlier is the presence of some spindle-shaped Fe-oxide particles (Figure 7d). Studying the clay fractions of the Oxisols used in this study, Padmanabhan and Mermut (1995) showed that these particles are magnetic and well-crystallized, consisting of Fe and Ti oxides. The presence of Ti-bearing particles was also proven by X-ray elemental mapping techniques, as previously discussed (Figure 4). Pore geometry is developed by

https://doi.org/10.1346/CCMN.1996.0440611 Published online by Cambridge University Press

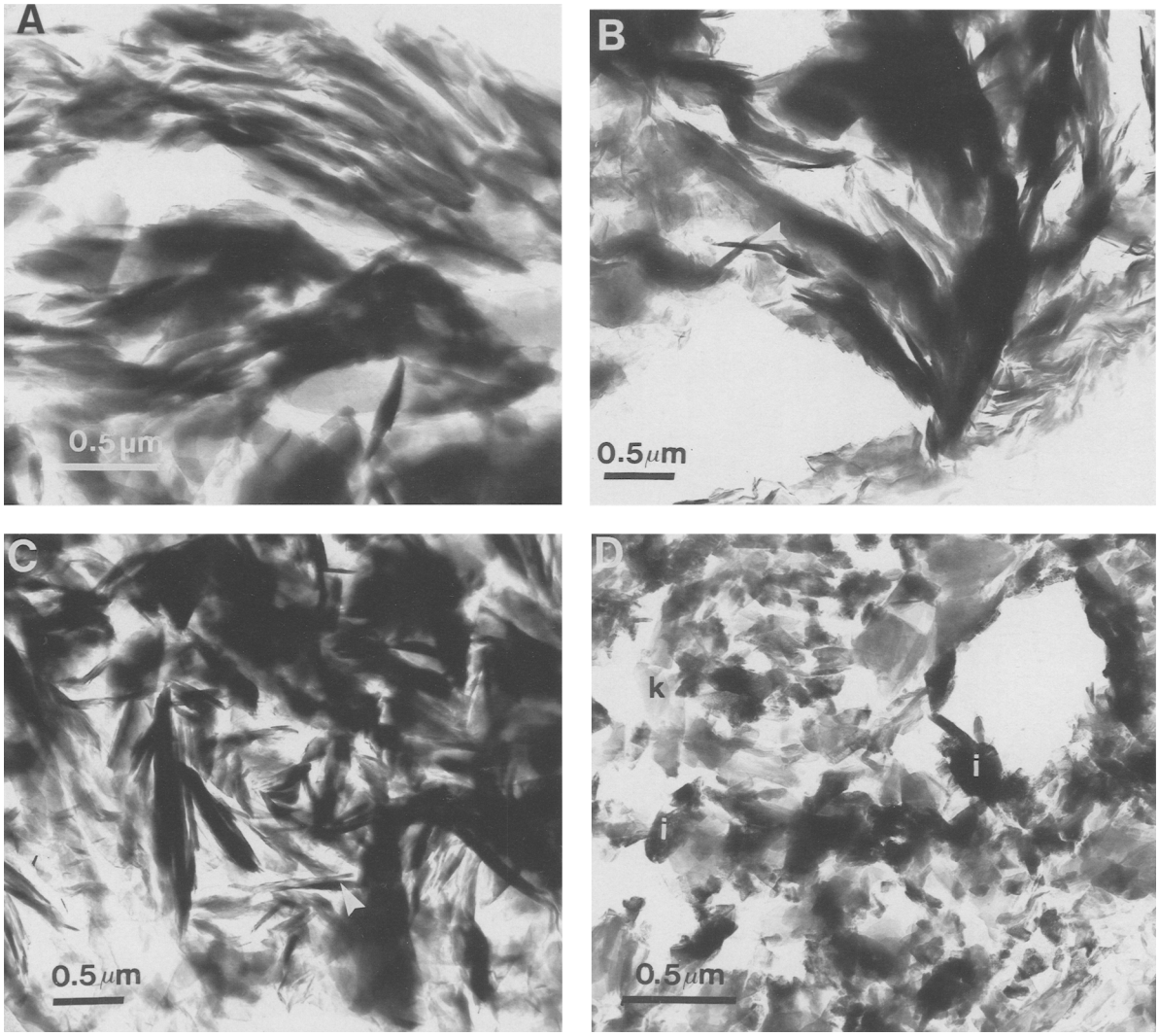

Figure 6. Transmission electron micrographs of ultra-thin sections: a) and b) from the edge of the coating; c) the various sizes of Fe-particles; and d) the transitional zone between the laminae and the central portion of the coating. i = Fe-oxides, k = kaolinite, arrows indicate smaller Fe-oxide particles.

random packing of strongly interconnected, individual grains sized mainly <0.5 µm (Figure 7). The abundance of voids differentiates the structure of this region from the laminae. The particle geometry of this region appears to be similar to that of soil microaggregates (Santos et al. 1989).

The formation of pure Fe-oxide laminae can be explained in terms of redox reactions. Compared to the laminae, the interior regions have lower concentrations and amounts of Fe-oxides. High porosity and low Fe-oxide content suggest that the Fe-oxides are mobilized by reducing conditions that exist in this region and that the reduced Fe^{2+} migrates towards the surface, where oxidation conditions exist. As the pore sizes are very small (<500 nm), it is likely that, under field conditions, the pores are filled by water, regardless of the moistness of the soil. The moisture available here would require a matric potential of >−1.5 MPa (Bui et al. 1989). In the initial stage, the porosity may have been lower than what is currently observed (under a much higher matric potential).

Considering the redox reactions (Krauskopf 1967), Fe-oxides can, under acid conditions, accept electrons from water molecules. They become reduced and mobilized, making the environment perhaps somewhat basic in pH, in comparison to the regular soil matrix:

$$Fe_2O_3 + 6H^+ + 2e^- \rightarrow 2Fe^{2+} + 3H_2O \quad [1]$$

However, when reduced Fe diffuses to the surface of the coating, oxidation reverses the reaction and H^+ is released to the environment, making the precipitation zone acid:

https://doi.org/10.1346/CCMN.1996.0440611 Published online by Cambridge University Press

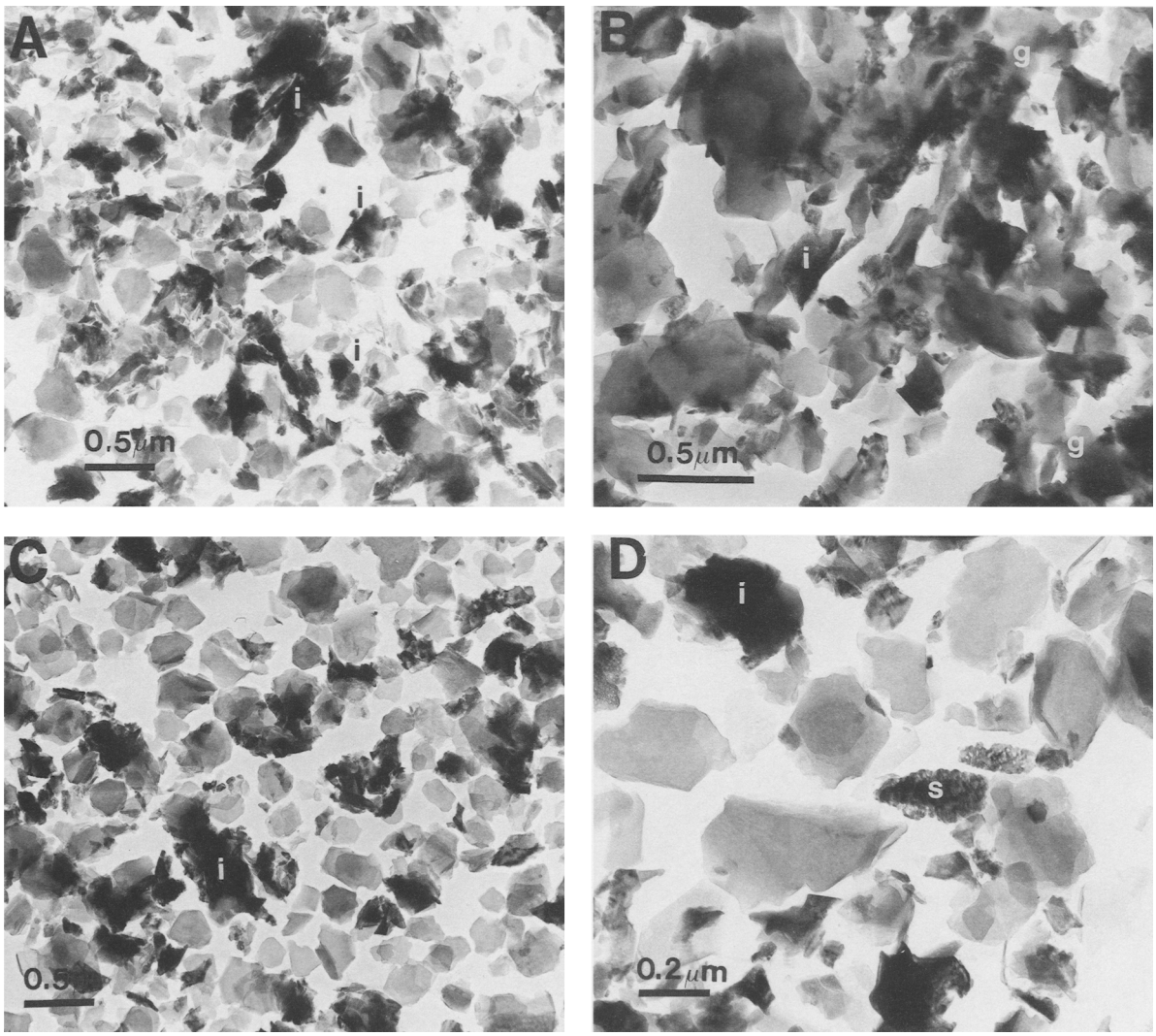

Figure 7. Transmission electron micrographs of the interlaminae regions: a) showing transition zone; b) gel-like coatings of Fe, Al and possibly Si in the transition zone; c) general submicroscopic fabrics of the interior regions at low magnification; and d) at higher magnification. Note differences in porosity, mineral assemblage and particle size between the various regions. i = Fe-oxides, s = spindle-shaped Fe-oxides.

$$Fe^{2+} + 3H_2O \rightarrow Fe(OH)_3 + 3H^+ + e^- \quad [2]$$

These reactions may be influential in the weathering of quartz (corrosion) and other mineral particles entrapped within the coating. Amouric et al. (1986) describe similar situations for the lateritic iron-crust pisolites from western Senegal. Wetting and drying of soil also influences the migration process.

As the Fe solubilized, dissolution voids were created and conditions for reduction may then have decreased. Surprisingly, the porosity observed within the interior regions of the Fe-oxide coating appears to be higher than that within the soil microaggregates of the same Oxisol studied by Santos et al. (1989). Considering the higher porosity and the concentration of Fe at the external part of the Fe-oxide coatings (Figures 3 and 4), the hypothesis regarding Fe migration from the centers of coatings appears to be plausible. This study shows that the size and geometry of the ultramicropores play a significant role in the dissolution and precipitation of soil minerals, especially those that exercise redox reactions.

The rigid surface of Fe-coatings would serve as a site for a new phase of Fe accumulation when the soil solution provides a new influx of iron, thereby increasing the thickness of the coating. The presence of several sets of Fe-laminae within the coatings seems to prove this view. The shape of discrete quartz and kaolinite grains suggests that they are stable in regions of high porosity and low Fe-oxide contents. Quartz and kaolinite are probably initially cemented by the

https://doi.org/10.1346/CCMN.1996.0440611 Published online by Cambridge University Press

Fe-oxides and remain within the coating. Sites that were covered by Al-oxides suggest that kaolinite (the major Al-bearing mineral in the system) has undergone a dissolution process, and/or that they were also engulfed during the formation of Fe-coatings. Large amounts of void spaces may have, in part, been formed by the dissolution of the quartz and kaolinite.

CONCLUSIONS

Ultramicroscopic analyses provided a window to observe the size, shape, orientation and distribution of the fundamental particles within the Fe-oxide coatings developed on quartz grains. The quartz surfaces served as nuclei for the formation of Fe-coatings. Changes in the physical chemistry in ultramicropores probably resulted in the corrosion of quartz grains. The contact zone with quartz and the edge of the coatings (laminae) are all composed of elongated Fe-oxide particles (up to 1.5 μm in length) arranged in a subparallel and compact manner. No other minerals exist in this region, which is <10 μm thick. The absence of Al and the dry soil environment favor the formation of large hematite particles in these very narrow zones.

The interior regions are composed of Fe-oxides, which are smaller in size and more rounded, together with kaolinite, quartz and some Ti-bearing minerals. It is likely that kaolinite, quartz and other minerals could have been trapped initially within the coating.

The marked increase in pore size (500 nm) in the interior and the presence of gel-like material close to the surfaces of the laminae (the transitional regions) suggest that Fe has been solubilized. This appears to be due to the nm pore size that created a very high matric potential (>−1.5 MPa) and reducing conditions within the Fe-coating, which caused the outward migration where oxidation conditions existed. This process appears to have helped the development of dense laminae. In addition to iron migration, voids may have been formed, at least in part, by the dissolution of kaolinite, quartz and other minor minerals. The low porosity at the edge provides rigidity to the coating and also controls the inward diffusion of soil solution. Iron continues to accumulate on the rigid surface, subsequently increasing the thickness of the Fecoatings.

The information obtained from the ultramicrotomy is pertinent to the further understanding of the behavior of fundamental mineral particles and physicochemical processes that occur in ultramicro sites of soils and sediments.

ACKNOWLEDGMENTS

This research was supported through the Operating Grant No. A 0464 from the Natural Sciences and Engineering Research Council of Canada, awarded to A.R. Mermut. The authors are grateful to the assistance provided by T. Bonli (SEM-Microprobe) and Y. Yukio (TEM) and to Dr. T.C. Lacalli for providing the microtome. Dr. D. Krinsley and Dr. J.B. Dixon are thanked for their critical reviews of this manuscript (Contribution No. R773).

REFERENCES

Amouric M, Baronnet A, Nahon D, Didier P. 1986. Electron microscopic investigations of iron oxyhydroxides and accompanying phases in lateritic iron-crust pisolites. Clays Clay Miner 34:45–52.

Arshad MA, St. Arnaud RJ. 1980. Occurrence and characteristics of ferromanganiferous concretions in some Saskatchewan soils. Can J Soil Sci 60:685–695.

Bascomb CL. 1968. Distribution of pyrophosphate-extractable iron and organic carbon in soils of various groups. J Soil Sci 19:251–268.

Brewer R. 1976. Fabric and mineral analysis of soils. Melbourne, FL: Robert E. Kriger. 482 p.

Bruemmer GW, Gerth J, Tiller KG. 1988. Reaction kinetics of the adsorption and desorption of nickel, zinc and cadmium by goethite: I. Adsorption and diffusion of metals. Soil Sci 39:37–52.

Bui EN, Mermut AR, Santos MCD. 1989. Microscopic and ultramicroscopic porosity of an Oxisol as determined by image analyses and water retention. Soil Sci Soc Am J 53: 661–665.

Bullock P, Fedoroff N, Jongerius A, Stoops G, Tursina T, Babel U. 1985. Handbook for soil thin section description. Wolverhampton, UK: Waine Research. 152 p.

Cescas MP, Tyner EH, Harmer RS. 1970. Ferro-manganiferous soil concretions: a scanning electron microscopic study of their micropore structure. Soil Sci Soc Am Proc 34:641–644.

Cho HD, Mermut AR. 1992. Evidence for halloysite formation from the weathering of ferruginous chlorite. Clays Clay Miner 40:608–619.

Eswaran H, Lim CH, Sooryanarayana V, Nordin Daud. 1978. Scanning electron microscopy of secondary minerals in Fe-Mn glaebules. In: Delgado M, editor. Soil micromorphology. Proceedings of the 5th international working meeting on soil micromorphology; Grenada, Spain. Grenada: Departmento de Edafologia, Univ de Granada. p 589–609.

Eswaran H, Stoops G. 1979. Surface textures of quartz in tropical soils. Soil Sci Soc Am J 43:420–424.

Eswaran H, Sys C, Sousa EC. 1975. Plasma infusion—a pedological process of significance in the humid tropics. Anales de Edafologia y Agrobiologia 34:665–673.

Gallaher RN, Perkins HF, Radcliffe D. 1973. Soil concretions: I. X-ray spectrograph and electron microprobe analysis. Soil Sci Soc Am Proc 37:465–469.

Gallaher RN, Perkins HF, Tan KH, Radcliffe D. 1973. Soil concretions: II. Mineralogical analysis. Soil Sci Soc Am Proc 37:469–472.

Ghabru SK, St. Arnaud RJ, Mermut AR. 1987. Liquid magnetic separation of iron-bearing minerals from sand fractions of soils. Can J Soil Sci 67:561–569.

Herbillon AJ, Tran VAJ. 1969. Heterogeneity in silicon-iron mixed hydroxides. J Soil Sci 20:223–235.

Jackson ML. 1973. Soil chemical analysis—advanced course. 2nd ed, 8th printing. Madison, WI: ML Jackson, Univ of Wisconsin. 895 p.

Jones RC, Uehara G. 1973. Amorphous coatings on mineral surfaces. Soil Sci Soc Am Proc 37:792–798.

Krauskopf KB. 1967. Introduction to geochemistry. New York: McGraw-Hill. 721 p

Lewis DG, Schwertmann U. 1979. The influence of aluminium on the formation of iron oxides: IV. The influence of (Al), (OH) and temperature. Clays Clay Miner 27:195–200.

McKeague JA, Day JH. 1966. Dithionite- and oxalate-extractable Fe and Al as aids in differentiating various classes of soils. Can J Soil Sci 46:13–22.

Mehra OP, Jackson ML. 1960. Iron oxides removal from soils and clays by a dithionite-citrate system buffered with sodium bicarbonate. Clays Clay Miner 7:317–327.

Milnes AR, Fitzpatrick RW. 1989. Titanium and zirconium minerals. In: Dixon JB, Weed SB, editors. Minerals in soil environments. 2nd ed. Madison, WI: Soil Science Society of America. p 1132–1205.

Mohr ECJ, van Baren FA, van Schuylenbourgh J. 1972. Tropical soils: a comprehensive study of their genesis. The Netherlands: Geuze Dordrecht. 481 p.

Nahon DB. 1991. Self-organization in chemical lateritic weathering. Geoderma 51:5–13.

Padmanabhan E, Mermut AR. 1995. The problem in expressing the specific surface areas of clay fractions. Clays Clay Miner 43:237–245.

Pawluk S, Dumanski J. 1973. Ferruginous concretions in a poorly drained soil of Alberta. Soil Sci Soc Am Proc 37: 124–127.

Plançon A, Giese RF, Snyder R. 1988. The Hinckley Index for kaolinites. Clay Miner 23:249–260.

Santos MCD, Mermut AR, Ribeiro MR. 1989. Submicroscopy of clay microaggregates in an Oxisol from Pernambuco, Brazil. Soil Sci Soc Am J 53:1895–1901.

Schwertmann U. 1985. Occurrence and formation of iron oxides in various pedoenvironments. In: Stucki JW, Goodman BA, Schwertmann U, editors. Iron in soils and clay minerals. NATO ASI Series C: Mathematical and Physical Sciences, vol 217. Boston: D. Reidel. p 267–308.

Schwertmann U, Fitzpatrick RW, Le Roux J. 1977. Al-substitution and differential disorder in soil hematites. Clays Clay Miner 25:373–374.

Schwertmann U, Fitzpatrick RW, Taylor RM, Lewis DG. 1979. The influence of aluminium on iron oxides: Part II. Preparation and properties of Al-substituted hematites. Clays Clay Miner 27:105–112.

Schwertmann U, Taylor RM. 1989. Iron oxides. In: Dixon JB, Weed SB, editors. Minerals in soil environments. 2nd ed. Madison, WI: Soil Science Society of America. p 379–438.

Shadfan H, Dixon JB, Calhoun FG. 1985. Iron oxide properties versus strength of ferruginous crust and iron-glaebules in soils. Soil Sci 140:317–325.

Sherman GD, Kanehiro Y. 1954. Origin and development of ferruginous concretions in Hawaiian Latosols. Soil Sci 77: 1–8.

Smart P, Tovey K. 1982. Electron microscopy of soils and sediments: techniques. Oxford: Clarendon Pr. 264 p.

Sposito G, Reginato RJ, editors. 1992. Opportunities in basic soil science research. Madison, WI: Soil Science Society of America. 109 p.

Spurr AR. 1969. A low-viscosity epoxy embedding medium for electron microscopy. J Ultrastruct Res 26:31–43.

Tardy Y, Nahon D. 1985. Geochemistry of laterites, stability of Al-goethite, Al-hematite, and Fe^{3+}-kaolinite in bauxites and ferricretes: an approach to the mechanism of concretion formation. Am J Sci 285:865–903.

Taylor RM, Schwertmann U. 1974. The association of phosphorous with iron in ferruginous soil concretions. Aust J Soil Res 12:133–145.

Tiessen H, Frossard E, Mermut AR, Nyamekye AL. 1991. Phosphorous sorption and properties of ferruginous nodules from semiarid soils from Ghana and Brazil. Geoderma 48: 373–389.

Trolard F, Tardy Y. 1989. A model of Fe^{3+}-kaolinite, Al^{3+}-goethite, Al^{3+}-hematite equilibria in laterites. Clay Miner 24:1–21.

Vempati RK, Loeppert RH, Sittertz-Bhatkar H. 1990. Infrared vibration of hematite formed from aqueous and dry thermal incubation of Si-containing ferrihydrite. Clays Clay Miner 38:294–298.

(Received 5 April 1995; accepted 22 February 1996; Ms. 2641)